# 1 Hybridized Orbital Ordering Project

## – Orbital hybridization ordering study in strongly correlated electron systems and the external field effect –

*Project Leader: Hironori Nakao*

### 1-1 Introduction

Strongly correlated electron systems (SCES) show various intriguing physical properties such as high $T_C$ superconductivity and colossal magnetoresistance effects near the metal–insulator transition, where itinerancy and localization of electrons compete with each other. For example, superconductors discovered in SCES generally exist in the vicinity of a quantum critical point. Hence, the study of the electronic state where itinerancy and localization of electrons compete is crucial for understanding the origin of these physical properties. There, the strong correlations among orbital, charge, and spin degrees of freedom also play important roles. Therefore the study of these electronic states is important for understanding the phenomena microscopically.

Resonant X-ray scattering (RXS) at the *K*-edge is a powerful tool for observing the spatial ordering of charge and orbital degrees of freedom in *3d* transition metal oxides. The RXS signal at the *K*-edge (*1s* → *4p* transition energy) reflects the *4p* electronic state. On the other hand, the RXS signal at the $L_{2,3}$-edge (*2p* → *3d* transition energy) can probe the *3d* electronic state directly, and the signal of resonant magnetic scattering is strongly observed at the $L_{2,3}$-edge of the *d* electron system. Moreover, *K*-edges of O, S, and P ions are also observable in the soft X-ray region. Namely, we can observe the localized electrons, *d*-electrons in transition metals and *f*-electrons in rare earth metals, and the itinerant electrons, O*2p*, P*3p*, and so on, by utilizing the resonant soft X-ray scattering (RSXS) technique, which is therefore key to elucidating the origin of physical properties in SCES.

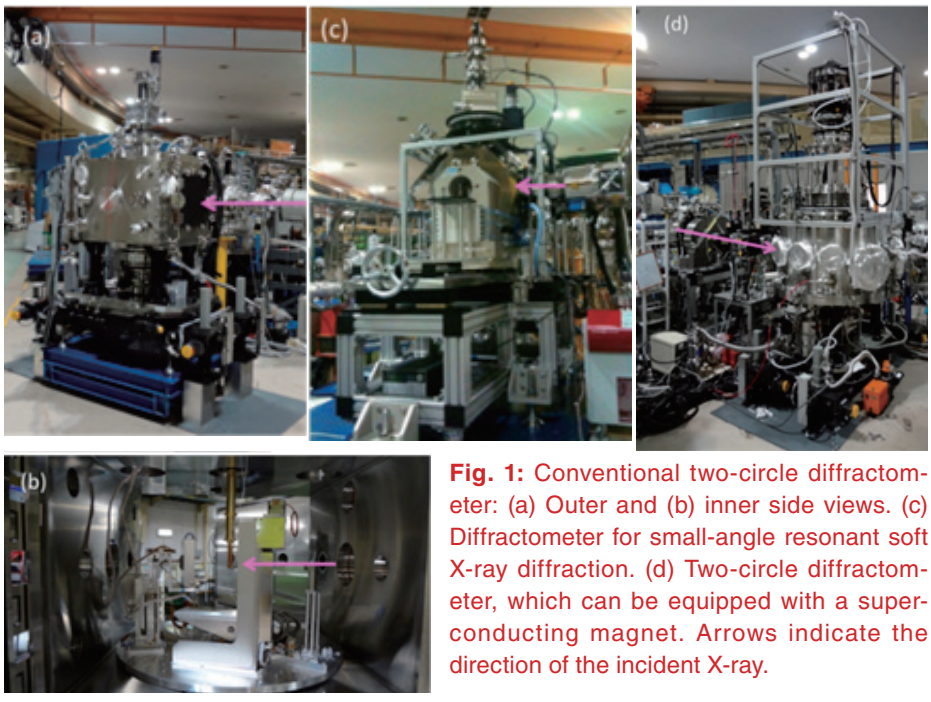


**Fig. 1:** Conventional two-circle diffractometer: (a) Outer and (b) inner side views. (c) Diffractometer for small-angle resonant soft X-ray diffraction. (d) Two-circle diffractometer, which can be equipped with a superconducting magnet. Arrows indicate the direction of the incident X-ray.

To perform the RSXS measurements, we have developed diffractometers to suit the experimental conditions. One is a conventional 2-circle diffractometer as shown in Fig. 1(a),(b) [1]. To use soft X-rays, the 4D-slit and detector must be placed on the 2θ table in a vacuum chamber. Hence, a diffractometer with a large vacuum chamber was built. The second diffractometer is specially designed for small-angle diffraction to detect spin textures (skyrmions, etc.) and domain structures (Fig.

1(c)) [2]. Finally, we have also developed a diffractometer with a superconducting magnet (< 7.5 T) to investigate the magnetic field effect of SCES (Fig. 1(d)) [3]. This diffractometer has the same geometrical configuration as that at BL-3A utilizing hard X-rays. Hence we can perform studies by complementary use of hard and soft X-rays. To detect weak resonant signals which reflect the change of physical properties in SCES, the detector development was very important, although conventional detectors exist for the hard X-ray region. First, we developed a silicon drift detector (SDD), which can detect just one photon. Moreover, the SDD has an energy resolution of < 100 eV, which enables us to reduce fluorescence background. As a result, we can detect weak signals sensitively. We also developed a two-dimensional X-ray detector – a CCD camera – for soft X-rays, which enables us to detect a wide $Q$ region by one exposure.

In order to conduct these RSXS experiments in this project, we needed a long beam time in the Photon Factory, because we needed to develop a diffractometer and detector for RSXS measurement, and the RSXS technique was expected to be used for many target materials. Hence this project has been performed by Special-2 proposals with the approval of the Photon Factory Program Advisory Committee (2009S2-008, 2012S2-005, and 2015S2-007).

The study of magnetic state is especially important in this project. The RSXS is an effective technique to detect magnetic signals, because the resonant signal directly reflects the *3d* electronic state utilizing the *2p* → *3d* dipole transition process at the $L_{2,3}$-edge. However, the observable range in scattering vector $Q$ is too narrow to completely determine the magnetic structure. On the other hand, neutron magnetic scattering measurement is a major technique for determining the magnetic structure, though a large amount of sample is needed for observation. As a result, complementary use of soft X-rays and neutrons is important here, and so neutron scattering experiments were performed [4-7] under the User Program for neutron scattering conducted by ISSP, The University of Tokyo, and under the approval of the Proposal Review Committee of J-PARC MLF (2010A0074).

In this project, the research encompassed various subjects such as transition metal oxides, rare earth metal compounds, and organic conductors, which are typical systems in SCES, and is being performed in collaboration with many external researchers. In this regard, cobalt oxides, which have spin-state degrees of freedom such as low-spin, high-spin, and intermediate-spin states, have been widely studied [8-13]. By controlling the spin-state, peculiar magnetic states have been found to emerge [10-13]. The other *3d* transition metal systems, V [4, 14], Cr [15, 16], Mn [5, 7, 17-19], Fe [20-22], and Ni [23], have also been investigated. Moreover, we have studied *4d* transition metal [24, 25], *f* electron [26, 27], and organic [28] systems. We have also discovered X-ray induced phase transitions as a by-product [17, 18]. As presented here, finally we have achieved scientific developments in each field. However, the key issue in this project, peculiar electronic states in which itinerancy and localization of electrons compete, is still being explored by utilizing the RSXS technique. In the near future, we expect to discover a key electronic state as an origin of a peculiar physical property in SCES. Here, we report the recent RSXS study of helical magnetic order and magnetic skyrmion crystal in B20-type cubic FeGe [22].

### 1-2 Formation of Skyrmion Crystal in FeGe as Probed by Small-Angle RSXS

The Dzyaloshinskii-Moriya interaction due to the breaking of inversion symmetry in the crystal lattice induces a topological spin texture in a ferromagnet, known as a magnetic skyrmion. The formation of skyrmion crystal (SkX), i.e. the triangular lattice of skyrmions [Fig. 2(a)], has been observed in bulk and thin films of chiral-lattice ferromagnetic alloys which lack inversion symmetry by small-angle neutron scattering (SANS) and Lorentz force microscopy [29, 30].

In this study, we observed the formation of SkX utilizing the small-angle RSXS technique. As shown in the schematic of the experimental geometry in Fig. 2(b), an in-vacuum CCD camera positioned downstream of the sample is utilized to record the resonant signal and a magnetic field of up to 0.5 T is applied parallel with the incident soft X-ray by a Helmholtz coil [Fig. 1(c)].

With this novel technique, we obtained CCD images of the small-angle RSXS for helical and SkX phases as shown in Fig. 3(a) and 3(b), respectively. The twofold symmetric arc-like magnetic peaks ($Q = \pm q_h$) come from the helical

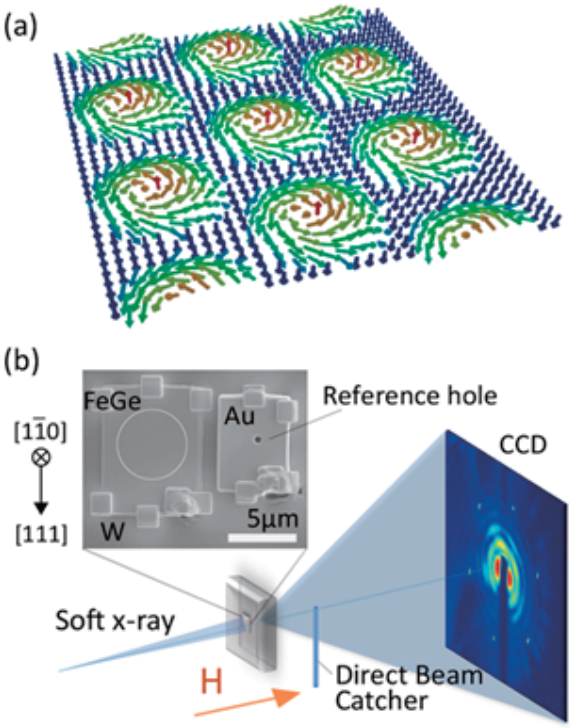


**Fig. 2:** (a) Schematic illustration of skyrmion crystal. (b) Schematic illustration of small-angle resonant X-ray scattering and picture of sample.

magnetic ordering, and the six-fold diffraction pattern ($Q = \pm q_1, \pm q_2, \pm q_3$) characteristic of the formation of SkX appears upon applying a magnetic field of 0.1 T. The present study reveals that the magnitude of the magnetic modulation vector in the helical phase ($|q_1|$) is slightly smaller than that in the SkX ($|q_h|$) due to the high angular resolution of resonant soft X-ray scattering, though it has been reported in the SANS study on FeGe that the magnitude of the q vector is coincident between the helical order and the SkX. In addition, a second-order magnetic scattering ($2q$) is also discerned in the SkX phase with weaker intensity by two orders of magnitude than the primary one ($q$), indicating that the deviation of the actual SkX from the simple triple-q configuration.

In this study, we also surveyed the dynamics upon the transformation between the helical and the SkX magnetic structure. As shown in Fig. 4, we measured magnetic scattering peaks with repeating magnetic field cycles between 0 and 0.1 T. Upon the transformation from helical to SkX phase with magnetic field applied, the rotation of SkX occurs concurrently with expanding lattice constant (decreasing $q$ value) of SkX. On the other hand, upon switching off the magnetic field, the SkX $q$ value abruptly increases and then starts to decrease in a few seconds, and finally

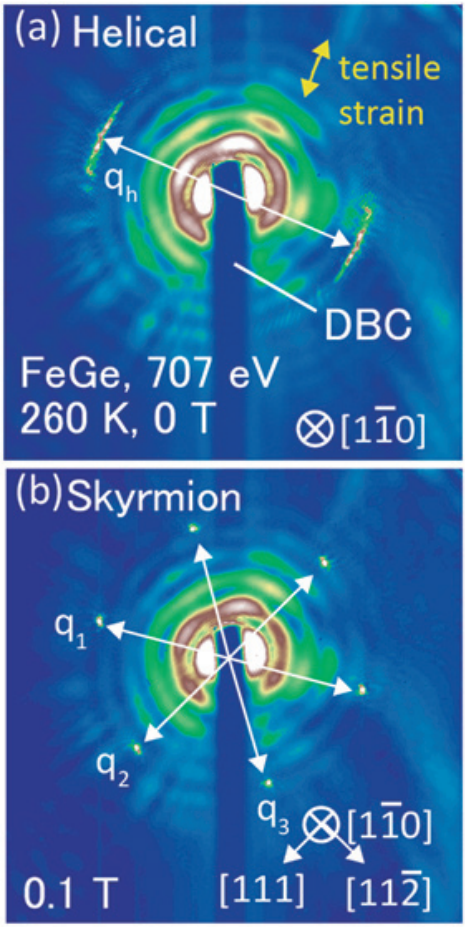


**Fig. 3:** CCD images of small-angle RSXS for (a) helical and (b) skyrmion crystal.

the SkX vanishes abruptly, transforming to the helical phase. Namely, abrupt shrinking of SkX occurs just after switching off the magnetic field and subsequent rotation and expansion of SkX occur. These results suggest that the expansion of lattice constant of SkX should be strongly coupled with the rotating motion of the SkX. The shrinking of the SkX may be forming micro-domains or clusters of skyrmions and then rotation of SkX may become possible within the individual domains, resulting in the apparent rotation of the whole SkX.

In conclusion, the helical magnetic structure and the SkX in FeGe were observed by small-angle magnetic scattering with soft X-ray resonant at the Fe *L*-edge. The high angular resolution magnetic reflections reveal the difference in the $q$ value between the helical order and the SkX, and also the transient motion of the SkX upon the change of magnetic field, such as the expansion of lattice constant and concurrent rotation of the SkX. Measurements using coherent and pulse soft X-ray will clarify the dynamics of skyrmions toward their application in spintronics.

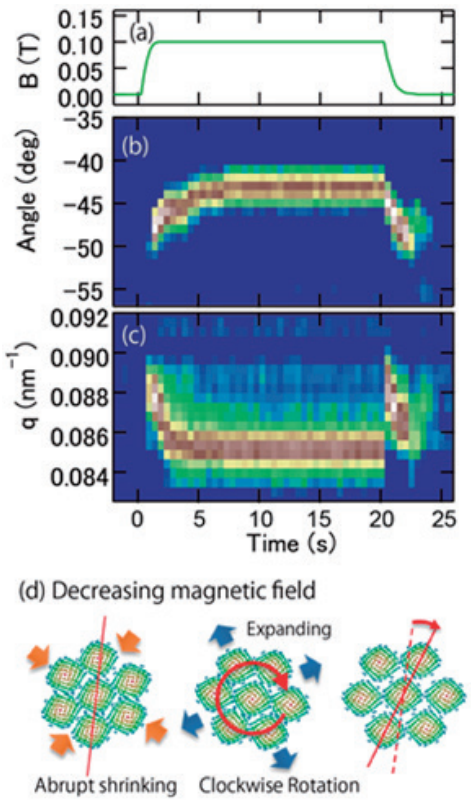


**Fig. 4:** Temporal change of (a) applied magnetic field, (b) the azimuthal angle $\varphi$, and (c) the magnitude of q vector of magnetic scattering from SkX magnetic structure. The schematic pictures show the transient variation in SkX structure from SkX to helical magnetic structure with decreasing magnetic field.

**Acknowledgements**

This project was partially supported by the JSPS KAKENHI Grant [Grant Nos. 16104005, 16684008, 21224008, 25286090], the Funding Program for World-Leading Innovative R&D on Science and Technology (FIRST), and the JST, Invitation for Applications for the Strategic Basic Research Programs (CREST).

References

[1] H. Nakao et al., J. Phys.: Conf. Ser. **502**, 012015 (2014).
[2] Y. Yamasaki et al., J. Phys.: Conf. Ser. **425**, 132012 (2013)
[3] J. Okamoto et al., J. Phys.: Conf. Ser. **502**, 012016 (2014);
[4] R. Fukuta et al., Phys. Rev. B **84**, 140409 (2011).
[5] H. Nakao et al., Solid State Commun. **185**, 18 (2014).
[6] Nakao et al., JPS Conf. Proc. **8**, 034010 (2015).
[7] H. Nakao et al., Phys. Rev. B **92**, 245104 (2015).
[8] J. Okamoto et al., J. Electron Spectrosco. Relat. Phenom. **184**, 224 (2011).
[9] J. Okamoto et al., J. Phys. Soc. Jpn. **83**, 044705 (2014).
[10] H. Nakao et al., J. Phys. Soc. Jpn. **80**, 023711 (2011).
[11] J. Fujioka et al., Phys. Rev. Lett. **111**, 027206 (2013).
[12] J. Fujioka et al., Phys. Rev. B **92**, 195115 (2015).
[13] Y. Yamasaki et al., J. Phys. Soc. Jpn. **85**, 023704 (2016).
[14] K. Takubo et al., Phys. Rev. B **86**, 085141 (2012).
[15] T. Toriyama et al., Phys. Rev. Lett. **107**, 266402 (2011).
[16] Nakao et al., J. Phys. Soc. Jpn. **81**, 054710 (2012).
[17] Y. Yamaki et al., Phys. Rev. B **87**, 081107(R) (2013).
[18] M. Kubota et al., Jpn. J. Appl. Phys. **53**, 05FH07 (2014)
[19] Y. Yamasaki et al., Phys. Rev. B **91**, 100403(R) (2015).
[20] T. Kobayashi et al., Phys. Rev. B **87**, 174520 (2013).
[21] T. Nakajima et al., Phys. Rev. B **91**, 205125 (2015).
[22] Y. Yamasaki et al., Phys. Rev. B **92**, 220421(R) (2015).
[23] M. Uchida et al., Phys. Rev. B **86**, 165126 (2012).
[24] R. Takahashi et al., J. Appl. Phys. **112**, 073714 (2012).
[25] S. Torigoe et al., Phys. Rev. B **93**, 085109 (2016).
[26] K. Iwasa et al., Phys. Rev. B **84**, 214308 (2011).
[27] K. Iwasa et al., JPS Conf. Proc. **3**, 016026 (2014).
[28] Y. Takahashi et al., J. Phys.: Conf. Ser. **502**, 012036 (2014).
[29] S. Mühlbauer, et al., Science **323**, 915 (2009).
[30] X. Yu, et al., Nature **465**, 901 (2010).